The *muX* project

F. Wauters[1⋆] and A. Knecht[2] on behalf of the *muX* collaboration[1]

1 PRISMA+ Cluster of Excellence and Institute of Nuclear Physics, Johannes Gutenberg Universität Mainz, Germany
2 Paul Scherrer Institut, Villigen, Switzerland
* Corresponding: fwauters@uni-mainz.de

January 29, 2021

PAUL SCHERRER INSTITUT

Review of Particle Physics at PSI
doi:10.21468/SciPostPhysProc.2

Abstract

The *muX* project is conducting a series of muonic X-ray measurements in medium- and high-Z nuclei at PSI, utilizing a high-purity germanium detector array, in-beam muon detectors, and a modern digital data-acquisition system. A novel hydrogen transfer target was developed, enabling measurements with as little as a few micrograms of target material. First measurements with radioactive Cm and Ra targets were conducted, aimed at determining their nuclear charge radii. These serve as important input for upcoming atomic parity violation experiments. The apparatus is also used to perform a feasibility study of an atomic parity violation experiment with the $2s-1s$ muonic X-ray transition. In addition, the setup has been made available for a wider range of nuclear, particle, and solid-state physics measurements.

22.1 Introduction

Muonic atoms are exotic atoms that form when negative muons are stopped in a target and are subsequently captured by a nearby atom in a highly excited atomic orbital, typically around n=14. The muons quickly cascade down to the 1s orbital, initially predominantly via Auger transitions: at lower n radiative transitions take over. As the muon mass is about 207 times larger than the electron mass, the muonic X-rays range in energy from a few tens of keV for low-Z nuclei to several MeV for heavier nuclei. The capture and cascade processes occur on (sub)nanosecond timescales. The emitted radiation therefore appears prompt relative to a muon stopping in the target. Once in the 1s orbit, the muon either decays in orbit, or is captured by the nucleus. The latter is the dominant decay channel for Z=12 and above [1].

Muonic atoms have proven to be a valuable tool to measure nuclear properties and probe short-range interactions between the muon and the nucleus. With the Bohr radius of the muon compared to the electron scaling as m_e/m_μ, there is substantial overlap between the muon and nuclear wave functions. Finite size effects are thus highly amplified. In the past, the absolute nuclear charge radii $< r^2 >^{1/2}$ of almost all stable nuclei have been determined with a typical accuracy of 10^{-4} - 10^{-3} by measuring the $2p-1s$ transition energy [2]. More recently, the radii of the lightest nuclei were measured by the CREMA collaboration (Section 21 [3]) using laser spectroscopy on muonic atoms [4–7].

Formerly, this approach was limited to stable isotopes, as a sufficient amount of target material is needed to stop a μ^- beam with a momentum of typically 30 MeV/c. This excludes

[1]https://www.psi.ch/en/ltp/mux

many interesting nuclei, such as the highly-deformed radium isotopes. Radium is a prime candidate for an Atomic Parity Violation (APV) experiment, using laser spectroscopy on a trapped ion [8,9], where the Parity Non-Conserving (PNC) $E1_{PNC}$ atomic $S-D$ transition is proportional to $K_r Z^2 Q_W$, with Q_W the weak nuclear charge, and K_r a relativistic enhancement factor which depends on the nuclear charge radius [10]. The *muX* collaboration aims to determine this radius by measuring the $2p-1s$ transition energy of ^{226}Ra ($T_{1/2}$=1600 y.). For this we have developed a novel technique, stopping muons in a high-pressure H_2/D_2 target, using a sequence of transfer reactions to efficiently stop muons in a few micrograms of target material. This technique was first established with gold targets, then applied to ^{226}Ra and ^{248}Cm (see Section 22.3).

With fundamental interactions being our primary physics motivation, the collaboration is also investigating the possibility of measuring APV directly in muonic atoms. A neutral parity-violating interaction mixes the $2s_{1/2}$ and $2p_{1/2}$ atomic levels, resulting in an E1 admixture in the otherwise pure M1 $2s_{1/2}-1s_{1/2}$ transition. Measuring such a parity-odd observable was first reviewed by Feinberg & Chen [11] and Missimer & Simons [12]. More recently, the possibility of searching for interactions between the muon and the nucleus beyond the Standard Model led to revived interest [13,14]. While the PNC effect is largest for low-Z atoms, separating the radiative M1/E1 transition from other transitions in the cascade severely complicates the design of such an experiment [15]. We focus on Z≃30 nuclei, where the single-photon $2s-1s$ transition becomes the dominant path depopulating the $2s$ level. The current goal of the collaboration is to isolate the transition in the cascade, and to significantly improve the signal-to-background ratio in the region-of-interest (ROI) in the X-ray spectrum (see Section 22.4.1).

Since 2015 we have been developing an advanced muonic X-ray experimental setup, combining a high-purity germanium (HPGe) detector array and a modern data-acquisition system (DAQ) with various target configurations. The setup is currently also being used for non-destructive elemental analysis, muon-capture studies probing matrix elements of interest for neutrinoless double β decay, and further nuclear-charge radius measurements of various radioactive elements and rare isotopes.

22.2 Experimental setup.

The *muX* apparatus (Figure 22.1 and Figure 22.2) is located at the πE1 beam-line of PSI, where a typically 30-40 MeV/c μ^- beam with a momentum width $\Delta p/p$ of 3 % passes through an electron separator before reaching the experiment. A custom beam snout houses an in-vacuum set of beam counters, thin plastic scintillator slabs read out by SiPMs, a lead target mounted away from the beam axis for calibration purposes, and a port for directly mounting various targets, thereby minimizing scattering of the low-energy muons.

The target itself is surrounded by 5 mm thick plastic scintillators, efficiently detecting outgoing decay electrons, thus enabling various cuts on the data such as suppressing Bremsstrahlung background in the HPGe detectors.

The *muX* HPGe detector array is constructed from various detectors provided by the collaborating institutions. Early campaigns, such as the $^{185/187}$Re measurement aimed at determining the charge radii and quadruple moments [16], were conducted with just a few coaxial HPGe detectors. For the 2017 and 2018 campaigns, 7 compact coaxial detectors from the French/UK loan pool[2] with relative efficiencies of around 60% and one Miniball cluster detector were added. In the summer of 2019, the full MiniBall detector array [17] was installed at the πE1 beamline (Figure 22.2), operating for a 7 week measurement campaign. The *muX* automatic liquid-nitrogen filling system enables extended continuous operation of the HPGe

[2] https://gepool.in2p3.fr/

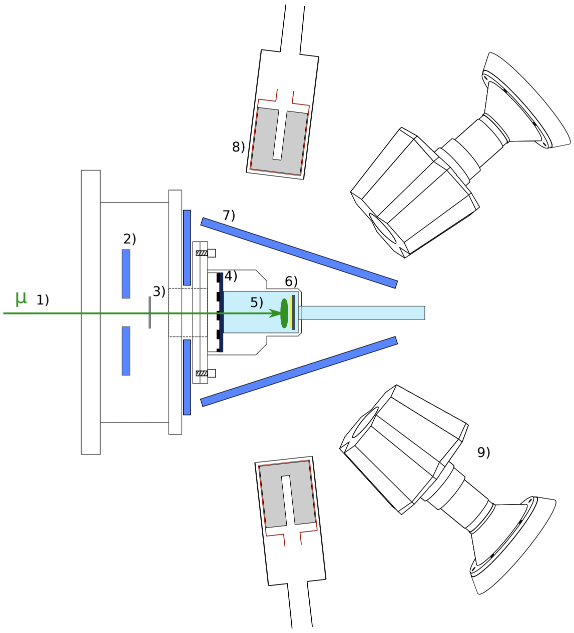

Figure 22.1: The muX setup, with 1) the μ^- beam passing through 2) a veto detector with a 18 mm aperture, and 3) a 200 μm thick muon detector. The cell 4) with a 600 μm carbon fibre window supported by a Ti grid holds 5) 100 bar of hydrogen gas, with the 6) target mounted in the back. 7) Electron veto detectors. 8) Standard and 9) MiniBall cluster HPGe detectors.

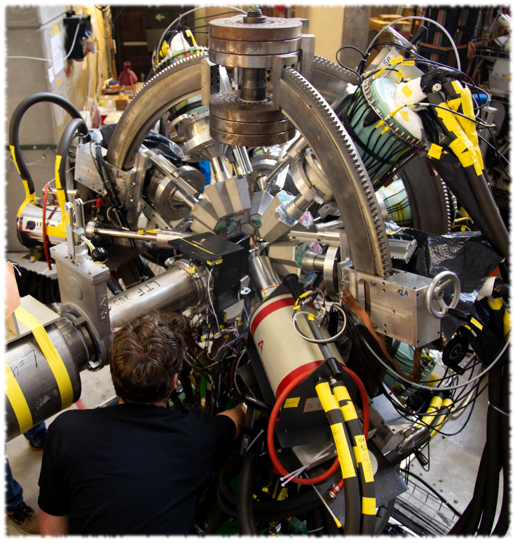

Figure 22.2: The MiniBall array with eight cluster detectors complemented by a 70 % coaxial detector and a low-energy planar detector installed at the πE1 beamline for the 2019 experimental run, with the muX beam snout. The target cell is covered by the black electron detectors.

detectors.

The MIDAS-based DAQ uses SIS3316 250 MSPS digitizers[3] which record all detector hits above threshold. Physics events are reconstructed offline by the analysis software. A digital filter running on the digitizer module FPGA integrates the detector signals, in addition, a section of the raw waveform is saved for offline analysis, where a time resolution of better than 10 ns (FWHM) for the HPGe detector hits is achieved.

22.3 Radioactive target measurements

One of the principal goals of the *muX* project [4] is to measure the $2p-1s$ transition energies for ^{226}Ra, a radioactive isotope for which the maximum allowed quantity in the experimental area is 5 μg. As the stopping power of such a low-mass target is insufficient by orders of magnitude, the *muX* collaboration has developed a novel method, stopping muons in a small 100 bar H_2 target with a small admixture of D_2. Through a series of transfer reactions the muon is transported to the target material mounted at the back of the cell (Figure 22.3), hereby exploiting the Ramsauer-Townsend effect [18–21], which causes H_2 gas to become almost fully transparent for a μd atom.

After a first optimization of the target geometry and conditions with Monte-Carlo simulations, the transfer method was established by mounting a thin gold target at the back of the

[3] https://www.struck.de/sis3316.html
[4] Proposal R-16-01

cylindrical gas cell. The beam momentum and deuterium concentration were optimized for the number of gold X-rays per muon, after which a small 3 nm thick gold target was installed. A total stopping efficiency per beam muon of 1.2 % was achieved for this 5 μg target (see Figure 22.4).

In order to have an efficient transfer target, it is imperative that the (radioactive) material is deposited as a uniform surface layer. Due to the low kinetic energy of the μd atom, an organic surface layer of >100 nm acts as a barrier and significantly reduces the transfer efficiency, rendering traditional molecular plating techniques inadequate. Several ^{248}Cm and ^{226}Ra targets were produced at the Institute of Nuclear Chemistry of the Johannes Gutenberg University Mainz, combining a custom electro-deposition technique combined with a novel *drop-on-demand* method where micro-drops of activity in solution are deposited on glassy carbon disks, the low-Z backing material of the target [22].

Figure 22.5 shows the muonic X-rays from ^{248}Cm measured during the 2019 campaign with a 15 μg curium target. After subtracting several background contributions, the $2p-1s$ transitions are clearly visible. Despite having nuclear ground state of spin 0, the energy scale of high-Z muonic atoms is such that the muon spin couples to excited nuclear states with a non-zero spin [23, 24]. This leads to a complicated dynamic hyperfine structure in the observed transition energies, which needs to be understood to extract the nuclear charge radius from the data. The largest uncertainty in the calculations of the transition energies is caused by the two-photon exchange nuclear polarization [25, 26].

In addition to the ^{248}Cm target, two ^{226} Ra targets were used. The data obtained are currently under analysis to determine whether the X-ray yield is sufficient to achieve the necessary accuracy on the nuclear charge radius.

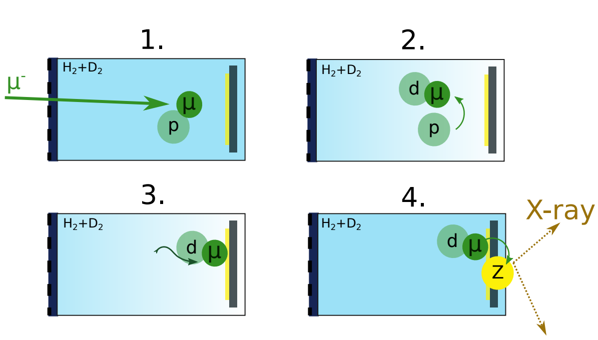

Figure 22.3: 1. After slowing down a μp atom is formed. 2. In $\mathcal{O}(100)$ ns, the muon transfers to deuterium, gaining 45 eV in kinetic energy. 3. After scattering down in energy to around 4 eV, the μd-H_2 scattering cross section becomes negligibly small, and the μd atom travels straight until it hits a wall or our target, where 4. the μ^- transfers to a high-Z atom.

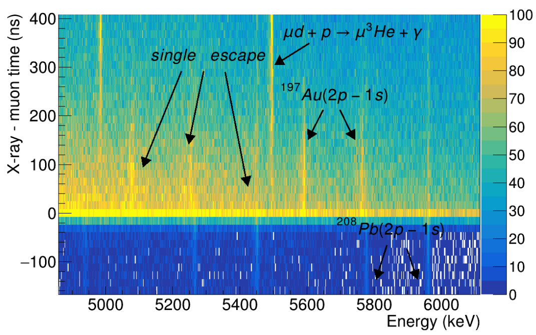

Figure 22.4: Muonic X-ray energies versus their time relative to an incoming muon. X-rays from direct stops appear at 0 ns. The Au X-rays appear over $\mathcal{O}(100)$ ns, the typical timescale for the transfer processes. The background mainly consists of decay electrons, and neutrons emitted after nuclear muon capture.

22.4 Extended experimental program

22.4.1 2s-1s measurements

With an expected branching ratio of $\mathcal{O}(10^{-4})$ for the single-photon $2s-1s$ muonic X-ray transition in the cascade of Z≃30 atoms, a possible APV experiment with a PNC observable using

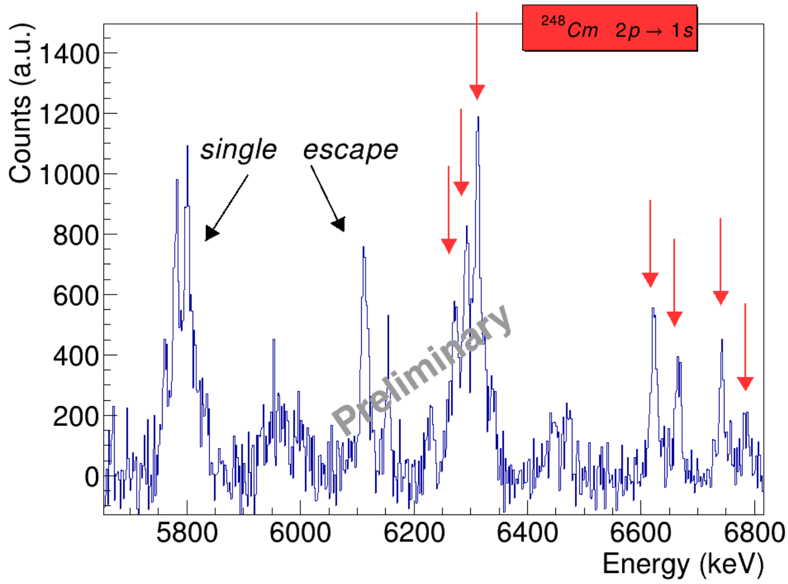

Figure 22.5: The ^{248}Cm muonic X-ray spectrum from the hydrogen transfer cell after subtracting the lead calibration lines and the γ background from muon capture on ^{16}O.

this transition is severely hampered by an overwhelming background in the energy region of interest (ROI) from scattered $(n \geqslant 3)p - 1s$ X-rays, Bremsstrahlung from decay electrons, and neutrons from muon capture. For this reason this transition has never been observed. The goal of the *muX* project is to observe this transition, significantly improve the signal-to-background in the ROI, and determine the reach of a possible APV experiment.

The initial average orbital quantum number l after $\mu H \rightarrow \mu Z$ transfer is lower than the initial l for direct atomic capture [27]. We have observed that as a consequence, the 2s population in the cascade of Ar, Kr, and Xe is increased by a factor of 3-4, thus increasing the branching ratio of the $2s - 1s$ transition. A 7 day measurement with a 100 bar H_2 target and an 0.1 % Kr addition was performed. After subtracting the nuclear capture background from muon stops in the surrounding materials, the $2s - 1s$ full energy peak is clearly visible, achieving a signal to background of about 1/10 (Figure 22.6).

To further reduce the background in the ROI, the transitions feeding the 2s level were used to tag events of interest. While sacrificing efficiency, this approach significantly reduces the background: the continuous Compton background from e.g. $3p - 1s$ photons is fully eliminated, and the accidental background from neutrons and decay electrons is at the same level as the signal yield, which can be further reduced by improving the time resolution. The only remaining challenging background is the satellite peaks introduced in the spectra by Compton scattered photons with energy depositions in the region of the 2s feeding transitions. This background needs to be controlled by optimizing the detector geometry. During the 2019 campaign, one week of data was taken with such an optimized geometry, collecting over 10^{11} muon stops on an isotopically pure ^{64}Zn target.

22.4.2 Other measurements

To fully benefit from the availability of the MiniBall detector array, the *muX* experimental program was expanded in 2019. The partial ordinary muon capture rates on enriched ^{130}Xe, ^{82}Kr, and ^{24}Mg to specific excited states in the daughter nucleus were measured. Such measurements provide valuable information to determine the nuclear matrix elements in neutrinoless

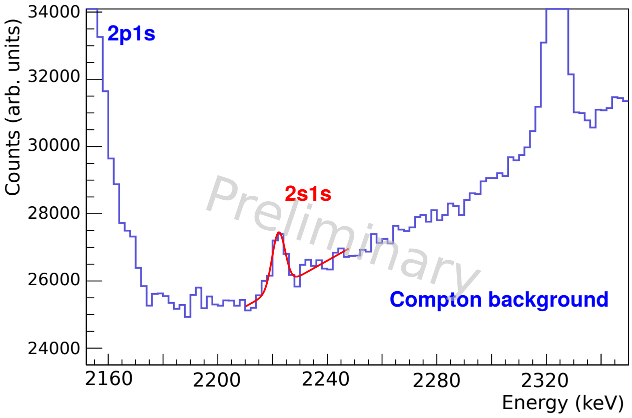

Figure 22.6: The $2s - 1s$ full energy peak clearly visible at 2.22 MeV above the Compton background of $(n > 2)p - 1s$ transitions after subtracting background γ's from nuclear muon capture processes.

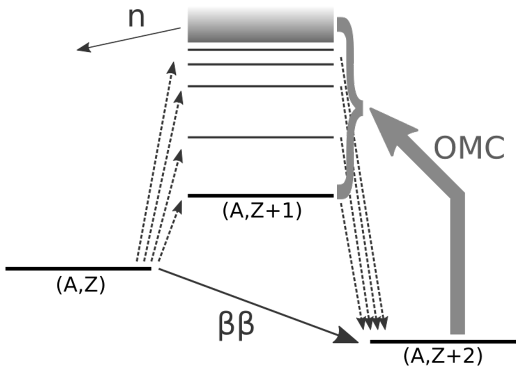

Figure 22.7: Partial muon capture rates of selected isotopes provide access to the transition strengths via virtual states in double β-decays.

double β-decay [28,29], as these states act as intermediate virtual states in the double β-decay of isotopes such as ^{130}Te [30,31] and ^{82}Se [32].

In addition, the *muX* apparatus was made available to perform elemental analysis on a series of cultural heritage samples, 17th century Japanese coins and an ancient Chinese mirror, significantly improving the sensitivity of previous J-PARC measurements [33], and a number of coins and recently found artifacts from the Roman Augusta Raurica site, nearby PSI. The intense muon beam and efficient detector setup permitted a narrowly collimated beam, probing different areas of a sample. Muonic X-ray spectroscopy provides information about the bulk material compared to the surface sensitivity of traditional fluorescence X-ray analysis. Furthermore, for high Z-elements such as lead the isotopic composition can be extracted.

22.5 Conclusions and Outlook

The *muX* efforts have resulted in a revived muonic X-ray program at the Paul Scherrer Institut. A new versatile experimental setup allows us to efficiently take data for extended periods of time.

The new hydrogen transfer target we have developed enables muonic X-ray measurements with a very small amount of target material. First measurements were performed with a Cm and Ra targets, with the purpose of extracting the nuclear charge radius, providing valuable input for upcoming APV experiments. The radioactive program will be extended to other elements, aiming to measure the third of three isotopes of odd Z-elements needed to calibrate the vast amount of isotope shift data available from laser spectroscopy on radioactive elements [34].

The single photon $2s - 1s$ transition in the muonic X-ray cascade was observed for the first time, and significant progress was made in reducing the backgrounds. This opens up the possibility for an APV experiment with a sensitivity of $\mathcal{O}(1)$ of the Standard Model amplitude, i.e., such a measurement would act as a new physics search.

The two additional measurements of the 2019 campaign, the OMC capture measurements and the elemental analysis, will continue as separate projects with the support of the *muX* collaboration.

Acknowledgements

This work was supported by the PSI through the Career Return Program, by the Swiss National Science Foundation through the Marie Heim-Vögtlin grant No. 164515 and the project grant No. 200021165569, by the Cluster of Excellence "Precision Physics, Fundamental Interactions, and Structure of Matter" (PRISMA EXC 1098 and PRISMA+ EXC2118/1) funded by the German Research Foundation (DFG) within the German Excellence Strategy (ProjectID 39083149), and by the DFG under Project WA 4157/1. We wish to thank all collaborating institutions providing essential instrumentation such as high-purity germanium detectors.

References

[1] T. Suzuki, D. F. Measday and J. P. Roalsvig, *Total nuclear capture rates for negative muons*, Phys. Rev. C **35**, 2212 (1987), doi:10.1103/PhysRevC.35.2212.

[2] G. Fricke, C. Bernhardt, K. Heilig, L. Schaller, L. Schellenberg, E. Shera and C. Dejager, *Nuclear ground state charge radii from electromagnetic interactions*, Atomic Data and Nuclear Data Tables **60**(2), 177 (1995), doi:https://doi.org/10.1006/adnd.1995.1007.

[3] A. Antognini, F. Kottmann and R. Pohl, *CREMA*, SciPost Phys. Proc. **2**, ppp (2021), doi:10.21468/SciPostPhysProc.2.XXX.

[4] R. Pohl *et al.*, *Laser spectroscopy of muonic deuterium*, Science **353**(6300), 669 (2016), doi:10.1126/science.aaf2468, http://science.sciencemag.org/content/353/6300/669.full.pdf.

[5] A. Antognini, F. Nez, K. Schuhmann, F. D. Amaro, F. Biraben, J. M. R. Cardoso, D. S. Covita, A. Dax, S. Dhawan, M. Diepold, L. M. P. Fernandes, A. Giesen *et al.*, *Proton Structure from the Measurement of $2S-2P$ Transition Frequencies of Muonic Hydrogen*, Science **339**, 417 (2013), doi:10.1126/science.1230016.

[6] R. Pohl *et al.*, *Laser Spectroscopy of Muonic Atoms and Ions*, JPS Conf. Proc. **18**, 011021 (2017), doi:10.7566/JPSCP.18.011021, 1609.03440.

[7] J. J. Krauth *et al.*, *Measuring the α-particle charge radius with muonic helium-4 ions*, nature **589**, 527 (2020), doi:10.1038/s41586-021-03183-1.

[8] M. Nuñez Portela *et al.*, *Towards a precise measurement of atomic parity violation in a single Ra^+ ion*, Hyperfine Interact. **214**(1-3), 157 (2013), doi:10.1007/s10751-013-0774-0.

[9] M. Fan, C. Holliman, A. Wang and A. Jayich, *Laser Cooling of Radium Ions*, Phys. Rev. Lett. **122**(22), 223001 (2019), doi:10.1103/PhysRevLett.122.223001, 1901.09882.

[10] L. W. Wansbeek, B. K. Sahoo, R. G. E. Timmermans, K. Jungmann, B. P. Das and D. Mukherjee, *Atomic parity nonconservation in ra^+*, Phys. Rev. A **78**, 050501 (2008), doi:10.1103/PhysRevA.78.050501.

[11] G. Feinberg and M. Chen, *The $2S_{(1/2)}\rightarrow 1S_{(1/2)}$ + 1 Photon Decay of Muonic Atoms and Parity Violating Neutral Current Interactions*, Phys. Rev. D **10**, 190 (1974).

[12] J. H. Missimer and L. M. Simons, *The Neutral Weak Current of the Muon*, Phys. Rept. **118**, 179 (1985).

[13] B. Batell, D. McKeen and M. Pospelov, *New parity-violating muonic forces and the proton charge radius*, Phys. Rev. Lett. **107**, 011803 (2011).

[14] D. McKeen and M. Pospelov, *Testing Parity with Atomic Radiative Capture of μ^-*, Phys.Rev.Lett. **108**, 263401 (2012).

[15] K. Kirch, D. Abbott, B. Bach, P. DeCecco, P. Hauser, D. Horváth, F. Kottmann, J. Missimer, R. T. Siegel, L. M. Simons and D. Viel, *Metastability of the muonic boron 2S state*, Phys. Rev. Lett. **78**, 4363 (1997), doi:10.1103/PhysRevLett.78.4363.

[16] A. Antognini, N. Berger, T. E. Cocolios, R. Dressler, R. Eichler, A. Eggenberger, P. Indelicato, K. Jungmann, C. H. Keitel, K. Kirch, A. Knecht, N. Michel *et al.*, *Measurement of the quadrupole moment of* ^{185}Re *and* ^{187}Re *from the hyperfine structure of muonic x rays*, Phys. Rev. C **101**, 054313 (2020), doi:10.1103/PhysRevC.101.054313.

[17] N. Warr *et al.*, *The Miniball spectrometer*, Eur. Phys. J. A **49**, 40 (2013), doi:10.1140/epja/i2013-13040-9.

[18] F. Mulhauser, A. Adamczak, G. A. Beer, V. M. Bystritsky, M. Filipowicz, M. C. Fujiwara, T. M. Huber, O. Huot, R. Jacot-Guillarmod, P. Kammel, S. K. Kim, P. E. Knowles *et al.*, *Ramsauer-townsend effect in muonic atom scattering*, Phys. Rev. A **73**, 034501 (2006), doi:10.1103/PhysRevA.73.034501.

[19] A. Adamczak and J. Gronowski, *Diffusion radius of muonic hydrogen atoms in H-D gas*, Eur. Phys. J. D **41**, 493 (2007), doi:10.1140/epjd/e2006-00252-6, physics/0609146.

[20] A. Adamczak, *Differential cross sections for muonic atom scattering from hydrogenic molecules*, Phys. Rev. A **74**, 042718 (2006), doi:10.1103/PhysRevA.74.042718, physics/0608243.

[21] P. Strasser, A. Taniguchi, T. Matsuzaki, K. Ishida, Y. Matsuda, S. Ohya, M. Iwasaki and K. Nagamine, *Muon spectroscopy with trace alkaline-earth and rare-earth isotopes implanted in solid D2*, Hyperfine Interact. **193**(1-3), 121 (2009), doi:10.1007/s10751-009-0055-0.

[22] R. Haas, S. Lohse, C. Düllmann, K. Eberhardt, C. Mokry and J. Runke, *Development and characterization of a drop-on-demand inkjet printing system for nuclear target fabrication*, Nuclear Instruments and Methods in Physics Research Section A: Accelerators, Spectrometers, Detectors and Associated Equipment **874**, 43 (2017), doi:https://doi.org/10.1016/j.nima.2017.08.027.

[23] D. Hitlin, S. Bernow, S. Devons, I. Duerdoth, J. W. Kast, E. R. Macagno, J. Rainwater, C. S. Wu and R. C. Barrett, *Muonic atoms. i. dynamic hyperfine structure in the spectra of deformed nuclei*, Phys. Rev. C **1**, 1184 (1970), doi:10.1103/PhysRevC.1.1184.

[24] N. Michel and N. S. Oreshkina, *Higher-order corrections to the dynamic hyperfine structure of muonic atoms*, Phys. Rev. A **99**, 042501 (2019), doi:10.1103/PhysRevA.99.042501.

[25] P. Bergem, G. Piller, A. Rueetschi, L. Schaller, L. Schellenberg and H. Schneuwly, *Nuclear polarization and charge moments of Pb-208 from muonic x rays*, Phys. Rev. C **37**, 2821 (1988), doi:10.1103/PhysRevC.37.2821.

[26] A. Haga, Y. Horikawa and Y. Tanaka, *Nuclear polarization in muonic Pb-208*, Phys. Rev. A **66**, 034501 (2002), doi:10.1103/PhysRevA.66.034501.

[27] P. Haff, E. Rodrigo and T. Tombrello, *Muon transfer in gas targets*, Annals of Physics **104**(2), 363 (1977), doi:https://doi.org/10.1016/0003-4916(77)90336-0.

[28] D. Zinatulina, V. Brudanin, V. Egorov, C. Petitjean, M. Shirchenko, J. Suhonen and I. Yutlandov, *Ordinary muon capture studies for the matrix elements in $\beta\beta$ decay*, Phys. Rev. C **99**, 024327 (2019), doi:10.1103/PhysRevC.99.024327.

[29] L. Jokiniemi and J. Suhonen, *Comparative analysis of muon-capture and $0\nu\beta\beta$ -decay matrix elements*, Phys. Rev. C **102**(2), 024303 (2020), doi:10.1103/PhysRevC.102.024303.

[30] D. Q. Adams, C. Alduino, K. Alfonso, F. T. Avignone, O. Azzolini, G. Bari, F. Bellini, G. Benato, M. Biassoni, A. Branca, C. Brofferio, C. Bucci *et al.*, *Improved limit on neutrinoless double-beta decay in* ^{130}Te *with cuore*, Phys. Rev. Lett. **124**, 122501 (2020), doi:10.1103/PhysRevLett.124.122501.

[31] S. Andringa *et al.*, *Current Status and Future Prospects of the SNO+ Experiment*, Adv. High Energy Phys. **2016**, 6194250 (2016), doi:10.1155/2016/6194250, 1508.05759.

[32] R. Arnold *et al.*, *Probing New Physics Models of Neutrinoless Double Beta Decay with SuperNEMO*, Eur. Phys. J. C **70**, 927 (2010), doi:10.1140/epjc/s10052-010-1481-5, 1005.1241.

[33] K. Ninomiya *et al.*, *Elemental Analysis of Bronze Artifacts by Muonic X-ray Spectroscopy*, JPS Conf. Proc. **8**, 033005 (2015), doi:10.7566/JPSCP.8.033005.

[34] B. Cheal, T. Cocolios and S. Fritzsche, *Laser spectroscopy of radioactive isotopes: Role and limitations of accurate isotope-shift calculations*, Phys. Rev. A **86** (2012), doi:10.1103/PhysRevA.86.042501.